

LA-UR-81-304

**MASTER**

**TITLE:** LOS ALAMOS FIELD-REVERSED CONFIGURATION (FRC) RESEARCH

**AUTHOR(S):** W. T. Armstrong, R. R. Bartsch, J. C. Cochrane,  
R. K. Linford, J. Lipson, K. F. McKenna, D. A. Platts,  
E. G. Sherwood, R. E. Siemon, and M. Tuszewski

**SUBMITTED TO:** U. S.-Japan Joint Workshop on Compact Toroids,  
Osaka, Japan, February 1981

**DISCLAIMER**

This document is a report of work performed by an agency of the United States Government. Neither the United States Government nor any agency thereof, nor any of their employees, makes any warranty, expressed or implied, or assumes any legal liability for the accuracy, completeness, or usefulness of any information, product, or process disclosed, or represents that its use would not infringe upon privately owned rights. Reference herein to any specific commercial product, process, or service by trade name, trademark, manufacturer, or otherwise, does not necessarily constitute or imply its endorsement, recommendation, or approval by the United States Government or any agency thereof. The views and opinions of authors expressed herein do not necessarily state or reflect those of the United States Government or any agency thereof.

University of California



By acceptance of this article, the publisher recognizes that the U.S. Government retains a nonexclusive, royalty-free license to publish or reproduce the published form of this contribution, or to allow others to do so, for U.S. Government purposes.

The Los Alamos Scientific Laboratory requests that the publisher identify this article as work performed under the auspices of the U.S. Department of Energy.

DISTRIBUTION OF THIS DOCUMENT IS UNLIMITED

**LOS ALAMOS SCIENTIFIC LABORATORY**

Post Office Box 1663 Los Alamos, New Mexico 87545

An Affirmative Action/Equal Opportunity Employer

Los Alamos Field-Reversed Configuration (FRC) Research

W. T. Armstrong, R. R. Bartsch, J. C. Cochran, R. K. Linford,  
J. Lipson, K. F. McKenna, D. A. Platts, E. G. Sherwood, R. E. Siemon,  
and M. Tuszewski

Los Alamos National Laboratory, Los Alamos, New Mexico 87545

ABSTRACT

Recent experimental results are discussed for a compact toroid produced by a field-reversed theta-pinch and containing purely poloidal magnetic fields. The confinement time is found to vary inversely with the ion gyro-radius and to be approximately independent of ion temperature for fixed gyro-radius. Within a coil of fixed radius, the plasmoid major radius  $R$  was varied by  $\sim 30\%$  and the confinement appears to scale as  $R^2$ . A semi-empirical formation model has been formulated that predicts reasonably well the plasma parameters as magnetic field and fill pressure are varied in present experiments. The model is used to predict parameters in larger devices under construction.

## I. Introduction

A field-reversed configuration (FRC) is a compact toroid that contains no toroidal field and in which the plasma current is carried by particles of small gyro-radius compared to the plasma dimensions. FRC's have been produced in the laboratory, using the field-reversed theta-pinch, since the early 1960's. A survey of the experimental literature is given in Ref. 1. In the relatively recent experiments, such as the Los Alamos FRX-A and FRX-B experiments started in 1977, lifetimes in the range of 10-100  $\mu$ sec are obtained, and the plasma is observed to be grossly stable for many Alfvén transit times. The geometry of the plasma with respect to the theta-pinch coil is shown in Fig. 1.

This paper is devoted to the presentation of recent results from the FRX experiments at Los Alamos and to a comparison of these results with a semi-empirical formation model. The organization of the material is as follows. Section II contains a discussion of recent stable period scaling experiments on FRX-B. Section III addresses the issue of equilibrium constraints on the FRC and the implications with respect to radial transport. In Sections IV and V, applications of the semi-empirical formation model to the new FRX-B data and to the FRX-C device (presently under construction) are considered.

## II. Recent FRX-B Scaling of the Stable Period

The  $n = 2$  rotational instability in field-reversed configurations, as has been noted in past work, may be attributed to the transfer of angular momentum through particle diffusion across the separatrix.<sup>2</sup> This origin of rotation requires that approximately one-half of the initially confined plasma be lost for the instability threshold to be exceeded. Previous measurements of particle inventory decay for a particular set of conditions are consistent with this prediction.<sup>1</sup>

The one-dimensional, Lagrangian, transport model of Hamasaki,<sup>3</sup> where the quasi-linear diffusion coefficient for the lower hybrid drift instability is used,<sup>4,5</sup> has indicated that the time for half the particle inventory to be lost across the separatrix scales with  $R^2/\rho_1$ , but is not a function of the ion temperature ( $R$  is the major radius and  $\rho_1$  is the ion gyro-radius). Past experimental work appeared to be consistent with this scaling prediction.<sup>1</sup> The present work has extended the formation of field-reversed configurations over a much larger range of fill pressures and with significantly higher confining fields making it possible to test  $R^2/\rho_1$  scaling over a broader set of

conditions. Though experimental limitations did not allow the maximum value of  $R^2/\rho_1$  to be significantly increased, the predicted scaling was again observed over the extended range of density, temperature, and magnetic field. It is essential to note, however, that for both theory and experiment, the theta-pinch coil radius was kept constant. The elicited scaling with  $R$  cannot, therefore, be directly applied to the prediction of confinement in larger devices.

An experimental scan, in which the field was varied at a fixed fill pressure, indicates that the stable period is very insensitive to the ion temperature when  $R^2/\rho_1$  is held approximately constant.

The present work was conducted on the FRX-B device.<sup>1</sup> The meter-long, 12.5-cm radius ( $r_c$ ), theta-pinch coil is driven by a recently enlarged capacitor bank of 78  $\mu$ f charged to 40 kV. Ten-percent mirror fields on-axis are produced at the end of the coil through shaping of the coil ends. The magnetic field rises in 2.6  $\mu$ sec from a bias field level of -3.0 kG to the maximum field value of approximately 13 kG. The field is then crowbarred, settles to about 9.5 kG at 10  $\mu$ sec and decays with a time constant of 150  $\mu$ sec. The plasma is pre-ionized with a 10- $\mu$ sec burst of RF at approximately 70 MHz, followed by a ringing theta-pinch discharge at approximately 500 kHz.

Figure 2 contains plots of the stable period,  $\tau_s$ , vs  $1/\rho_1$  and  $R^2/\rho_1$  for all FRX experiments to date. The quantity  $R$  is determined from excluded flux measurements in the axial midplane using  $r_{\Delta\phi} = r_s$  and  $r_s = \sqrt{2}R$  ( $r_{\Delta\phi}$  is the excluded flux radius<sup>1</sup> and  $r_s$  is the separatrix radius). The first relation requires straight field lines and the absence of plasma pressure on open field lines. These assumptions have been found to be well justified.<sup>1</sup> The second relation follows from radial pressure balance and equilibration of plasma pressure on flux surfaces.

The ion gyro-radius is calculated with respect to the external magnetic field. The ion temperature was determined from Doppler broadening of the 2271 Å line of carbon V. The polychromator used in this measurement viewed the plasma along a diameter in the axial midplane.

The most satisfactory scaling is  $\tau_s = 6.0 \times 10^{-7} R^2/\rho_1$  with  $\tau_s$  in sec,  $R$  and  $\rho_1$  in cm. It must be pointed out that the value of  $R$  varied by no more than 30% for these data while  $\rho_1$  varied by a factor of 4; thus, the scaling with respect to  $\rho_1$  is much more definitive than with respect to  $R$ . It is, however, noteworthy that the inclusion of the  $R^2$  factor considerably reduces the scatter in the data.

The convenient use of  $R$  in parameterizing the FRC should not obscure the fact that the transport is determined by the detailed radial density profile. Particularly significant are the density gradient length ( $\ell_n = (\frac{1}{n} \frac{dn}{dr})^{-1}$ ) and the density ( $n_s$ ) evaluated at the separatrix. It is the relative size of the ion gyro-radius at  $r_s$  compared to  $\ell_n$  and the magnitude of  $n_s$  that govern the diffusive loss of particles across the separatrix. For given values of  $R$ ,  $\rho_1$ , and  $R/r_c$ , the radial density profile is theoretically determined by pressure balance and particle transport. Thus, in a coil with fixed  $r_c$ , the readily determined variables  $R$  and  $\rho_1$  are apparently sufficient to establish  $\ell_n$  and  $n_s$ , and consequently, the confinement scaling.

Experiments were undertaken in which the external magnetic field,  $B$ , was varied by changing the main-bank charge voltage. The  $D_2$  filling pressure was held constant at 17 mTorr. It is found that for these data,  $\rho_1$  is approximately invariant and, to an even better approximation, so is  $R^2/\rho_1$ . With or without the small variations in  $R^2/\rho_1$  taken into account, it is apparent in Fig. 3 that  $\tau_s$  is virtually independent of ion temperature for  $200 \text{ eV} < T_i < 1200 \text{ eV}$ .

### III. FRC Equilibrium constraints on Radial Transport

Radial transport of particles is a crucial issue for FRC plasmas. In the absence of MHD instabilities, it limits the lifetime of the configuration and, as discussed above, it may be responsible for the onset of the destructive  $n = 2$  instability. The balance between plasma pressure and field line tension in an elongated 2-D equilibrium requires<sup>1</sup>

$$\langle \beta \rangle = 1 - \frac{1}{2} x_s^2 \quad (1)$$

where  $\langle \beta \rangle$  is the average  $\beta = p/(B^2/2\mu_0)$  over the separatrix volume, and where  $x_s$  is the ratio of separatrix to conducting wall radius. Eq. (1) suggests that for present typical values of  $x_s$  (0.4-0.5) the average  $\beta$  must be of order unity, which necessarily implies a fairly flat radial density profile with very steep density gradients in the vicinity of the separatrix since the open field line plasma is poorly confined. Radial transport (possibly of anomalous nature) may be increased substantially by these strong density gradients. Thus, it may be desirable to make  $x_s$  as large as possible in order to minimize pressure gradients, as suggested by Eq. (1). There is experimental evidence<sup>6</sup> that this

approach can result in long-lived FRC's. Alternatively, it may be possible to improve the confinement of plasma on open field lines by some means such as multiple mirrors, and thereby reduce the pressure gradient at the FRC boundary.

In order to increase  $x_g$ , one has to increase the amount of trapped flux  $\phi_1 = \int_0^R B_z 2\pi r dr$  of the FRC. The largest possible flux that can be trapped is  $\phi_0 = \pi r_t^2 B_1$ , where  $r_t$  is the inner radius of the discharge tube and  $B_1$  is the magnitude of the bias field. Pre-ionization, field reversal, implosion and formation of the 2-D equilibrium may all contribute to loss of trapped flux. For the recent FRX-B experimental results described in Section II of this paper, one can infer a value for  $\phi_1/\phi_0$  of about 0.13. The loss of flux implied by  $\phi_1/\phi_0$  can be explained in part by anomalous resistivity during the implosion phase according to numerical modeling.<sup>7,8</sup> Pre-ionization processes also appear to be important<sup>9</sup> and improved pre-ionization schemes at larger values of bias field are under study<sup>10</sup> to increase the final value of  $\phi_1/\phi_0$  and, therefore,  $x_g$ .

#### IV. Scaling Laws for FRC Formation

A semi-empirical method has been developed<sup>11</sup> to extrapolate the experimental results of past FRX-B work<sup>1</sup> to new similar experiments. The model uses dimensionless empirical constants,  $x_h$  to scale the implosion heating phase,  $x_f$  (equal to  $\phi_1/\phi_0$ ) for the trapped flux,  $x_b$  as the ratio of bias field to a maximum value first identified by Green and Newton<sup>12</sup> and  $x_p$  as the fraction of the initial particles contained in the formed equilibrium. From FRX-B data, the values of these constants are fixed to 0.06, 0.13, 0.75, and 0.35, respectively. For a given device and fill pressure  $P_0$ , the model predicts the temperature ( $T_e + T_i$ ), density, external confining field ( $B$ ), ratio of major radius  $R$  to ion gyro-radius  $\rho_i$  ( $S$ ) and the plasma dimensions ( $x_g$  and  $x_z = L_{\text{plasma}}/L_{\text{coil}}$ ) for an elongated 2-D equilibrium.

For the recent high-field operation of FRX-B described in the first part of this paper, the experimental values of  $x_g$ ,  $T_e + T_i$ ,  $B$  and  $S$  are obtained for various values  $P_0$ , 10  $\mu\text{sec}$  after the initiation of the main bank. The ion temperature is measured directly by CV broadening measurements, but the electron temperature is assumed to be 150 eV based on Thomson scattering measurements previously made under similar conditions.<sup>1</sup> These values, with typical error bars, (averaged over several shots) are plotted in Fig. 4, along with the predictions of the model for this particular experiment. One observes from Fig. 4 that there is a reasonable agreement between the results of the model and

the experimental values, except for the length of the configuration ( $z_g$ ) which is predicted to be in the range 0.3 to 0.5. Data (not included in Fig. 4) from an axial array of excluded flux loops indicate  $z_g \sim 0.8 \pm 0.2$ , with no noticeable dependence on  $P_0$ . The otherwise generally good agreement gives us some confidence that the model can be used to estimate the parameters of future experiments, in particular those of FRX-C.

#### V. The FRX-C Experiment

The main goal of FRX-C is to test the confinement scaling of an FRC of larger dimensions over a wide range of temperatures. The predicted parameters of FRX-C are given by comparison to those of FRX-B in Table I. As seen from Table I, the larger coil diameter (and, therefore, larger  $R$  at fixed  $x_g$ ) should allow a substantial extension of the FRC confinement scaling with  $R/\rho_1$  and also test the possible stability limits as the ratio of plasma size to ion gyro-radius increases. The larger bank and loop voltage (110 kV against 45 kV for FRX-B) are required to obtain adequate temperature over a wide range of  $P_0$  and enough adiabatic compression to contain the plasma within the coil length. A dual feed was chosen to achieve the effective 110 kV voltage on the theta-pinch coil with the same spark-gap technology as for FRX-B. The first operation of FRX-C is scheduled for May 1981.

Plotted in Fig. 5 are predictions of FRX-C parameters based on the previously described formation model and the device parameters corresponding to the case of Table J. One observes from Figs. 4 and 5 that the expected values for  $x_g$  are in the same range (0.4 to 0.5) as for the FRX-B experiment, which reflects the fact that the same fraction of trapped flux ( $\phi_1/\phi_0 \sim 0.13$ ) has been assumed in both cases. Larger values of  $x_g$  would be achieved if one can increase the final value of  $\phi_1/\phi_0$ . One also observes from Figs. 3 and 4 the substantial increase in the range of  $S$  achievable in FRX-C by comparison with FRX-B. Even larger values of  $S$  could be achieved if the trapped flux fraction exceeds the value of 0.13 assumed in these calculations.

Table I

<u>Parameters</u>	<u>FRX-B</u>	<u>FRX-C</u>
coil diameter	25 cm	45 cm
coil length	100 cm	200 cm
discharge tube i.d.	20 cm	40 cm
source voltage	40 kV	110 kV
B-field swing	16 kG	16 kG
1/4 period time	2.6 $\mu$ sec	5 $\mu$ sec
crowbar time	150 $\mu$ sec	300 $\mu$ sec
bank energy	62 kJ	510 kJ



References

1. W. T. Armstrong, R. K. Linford, J. Lipson, D. A. Platts, and E. G. Sherwood, Phys. Fluids (to be published).
2. D. C. Barnes and C. E. Seyler, in Proceedings of the U.S.-Japan Joint Symposium on Compact Toruses and Energetic Particle Injection (Princeton, 1979), p. 110.
3. S. Hamasaki and N. A. Krall, Conference Record IEEE International Conference on Plasma Science (Montreal) 5E10 (1979).
4. R. C. Davidson and N. A. Krall, Nucl. Fusion 17 1313 (1977).
5. T. T. Lee and J. F. Drake, Bull. Am. Phys. Soc. 25, 988 (1980).
6. A. G. Es'kov, in Plasma Physics and Controlled Nuclear Fusion Research (Proc. 7th Int. Conf. Innsbruck, 1978) Vol. 2, IAEA, Vienna (1979) 187.
7. W. T. Armstrong, et al., Third Symposium on Physics and Technology of Compact Toroids in the Magnetic Fusion Energy Program, Los Alamos 1980, Los Alamos National Laboratory Report LA-8700-C (1981), 180.
8. A. G. Sgro, Third Symposium on Physics and Technology of Compact Toroids in the Magnetic Fusion Energy Program, Los Alamos 1980, Los Alamos National Laboratory Report LA-8700-C (1981), 169.
9. W. T. Armstrong, et al., Appl. Phys. Letters (to be published).
10. R. J. Comisso, et al., Third Symposium on Physics and Technology of Compact Toroids in the Magnetic Fusion Energy Program, Los Alamos 1980, Los Alamos National Laboratory Report LA-8700-C (1981), 184.
11. R. E. Siemon and R. R. Bartsch, Third Symposium on Physics and Technology of Compact Toroids in the Magnetic Fusion Energy Program, Los Alamos 1980, Los Alamos National Laboratory Report LA-8700-C (1981), 172.
12. T. S. Green and A. A. Newton, Phys. Fluids 9, 1386 (1966).

Figure Captions

Figure 1. The FRC is seen inside the theta-pinch coil. The axial vectors are magnetic field lines and the azimuthal vectors show the direction of the plasma currents.

Figure 2. The value of  $\tau_g$  is plotted a) vs  $1/\rho_1$  and b) vs  $R^2/\rho_1$  for all FRX experiments to date. Each data point is representative of not less than 5 shots and typical rms deviations for  $\tau_g$ ,  $1/\rho_1$ , and  $R^2/\rho_1$  were 5%.

Figure 3. The value of  $\tau_g$  and  $\tau_g/(R^2/\rho_1)$  is plotted vs  $T_1$ . The data represent the same shots as in Fig. 2. The rms deviations in  $\tau_g$  and  $\tau_g/(R^2/\rho_1)$  do not exceed 10%.

Figure 4. Formation model predictions for FRX-B as a function of fill pressure  $P_0$ . Experimental data points are indicated for comparison.

Figure 5. Formation model predictions for FRX-C as a function of fill pressure  $P_0$ .

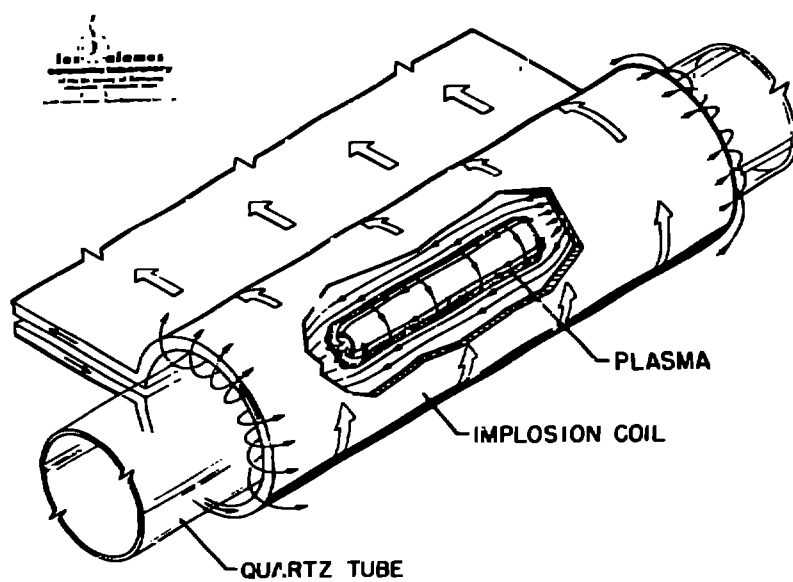
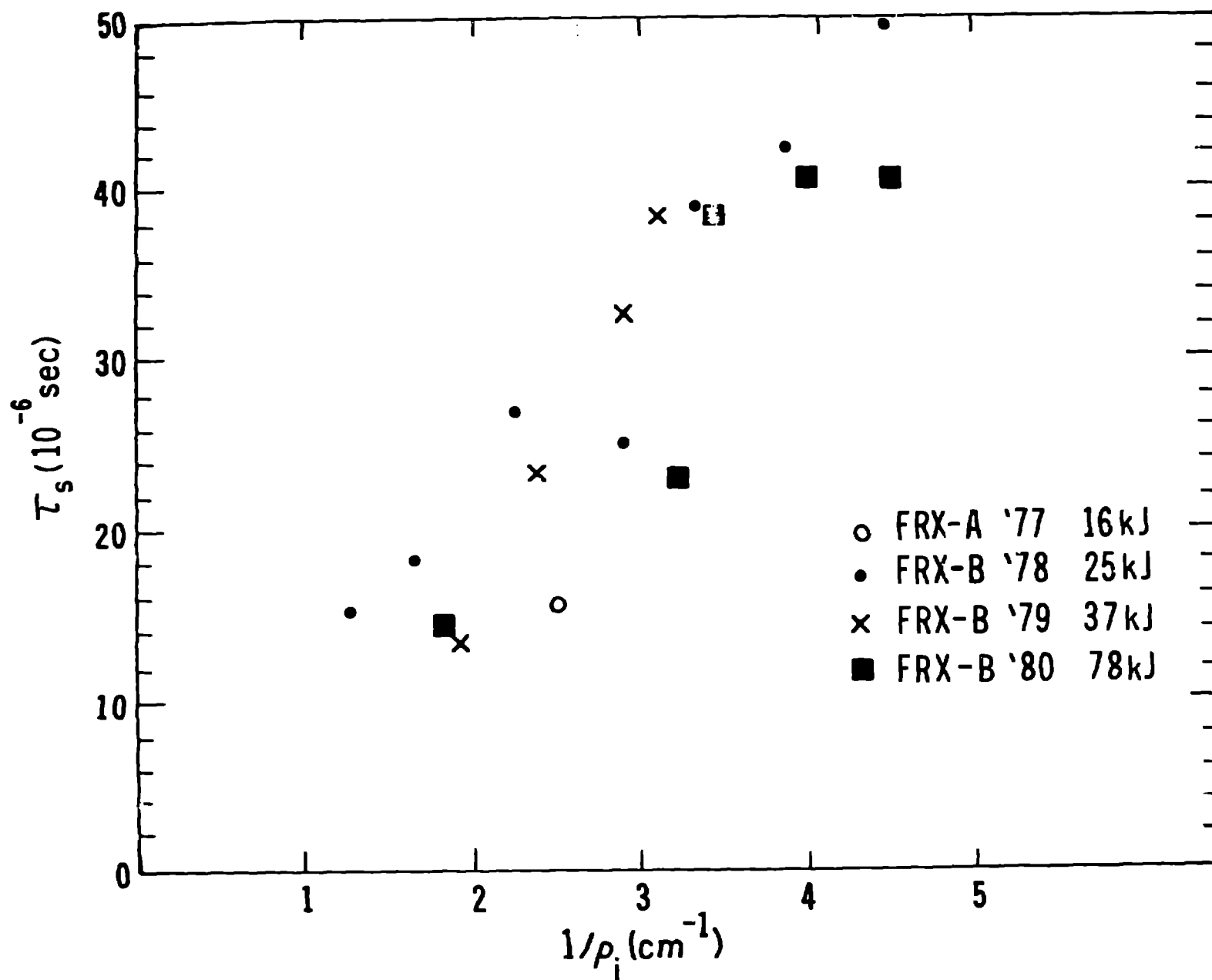
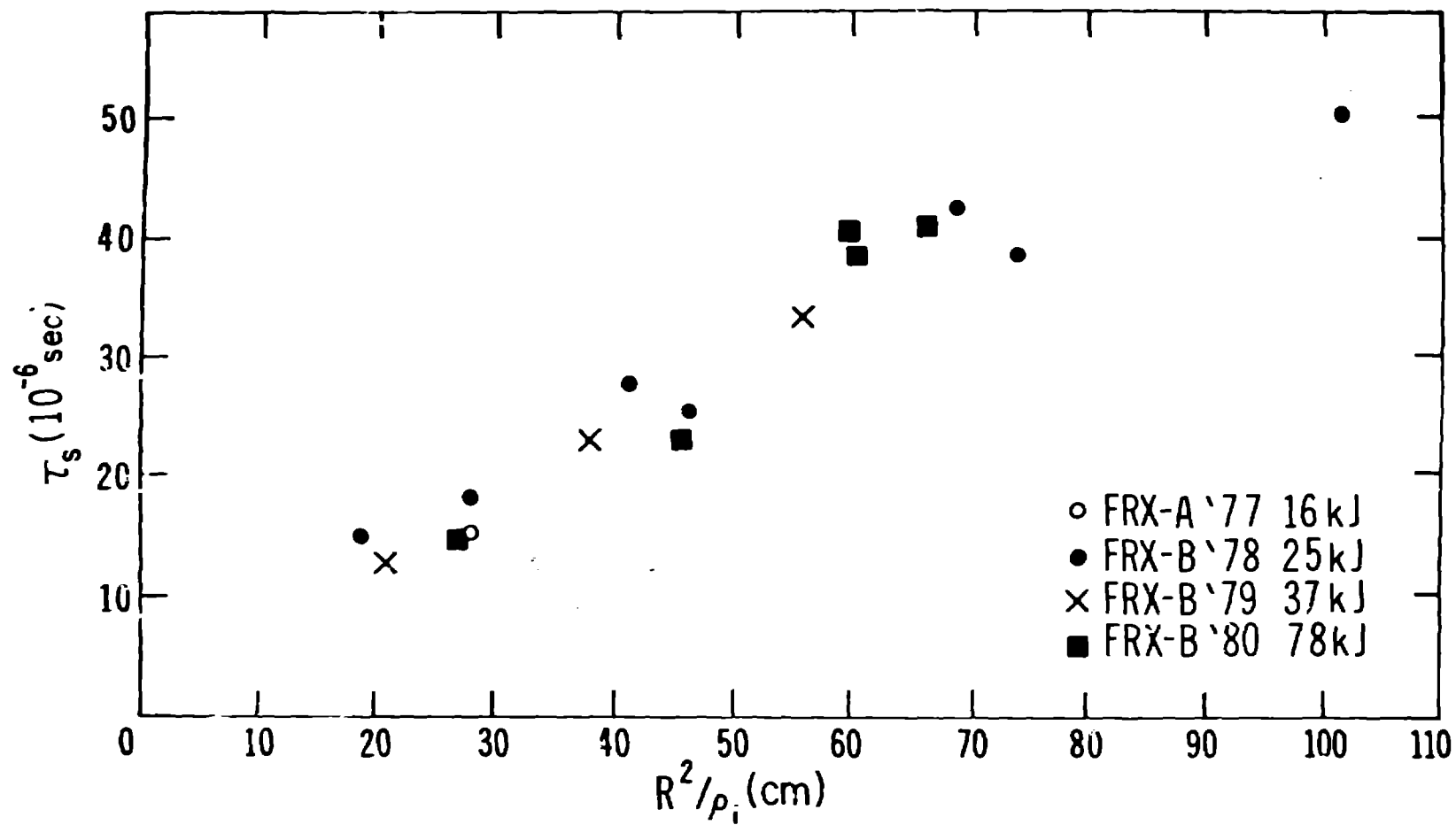


Fig. 1

Fig. 2a



FR. 2b



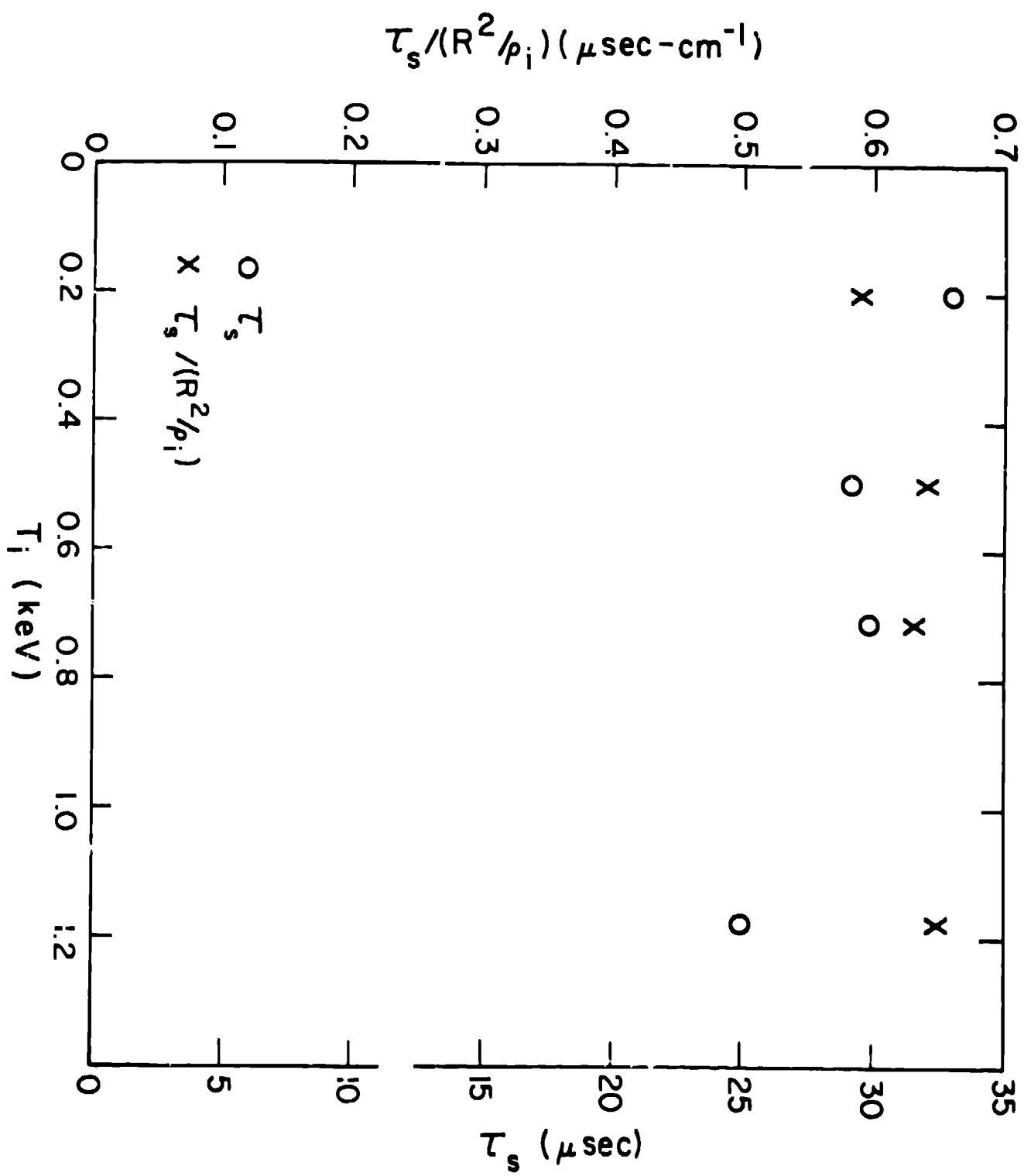


Fig. 3

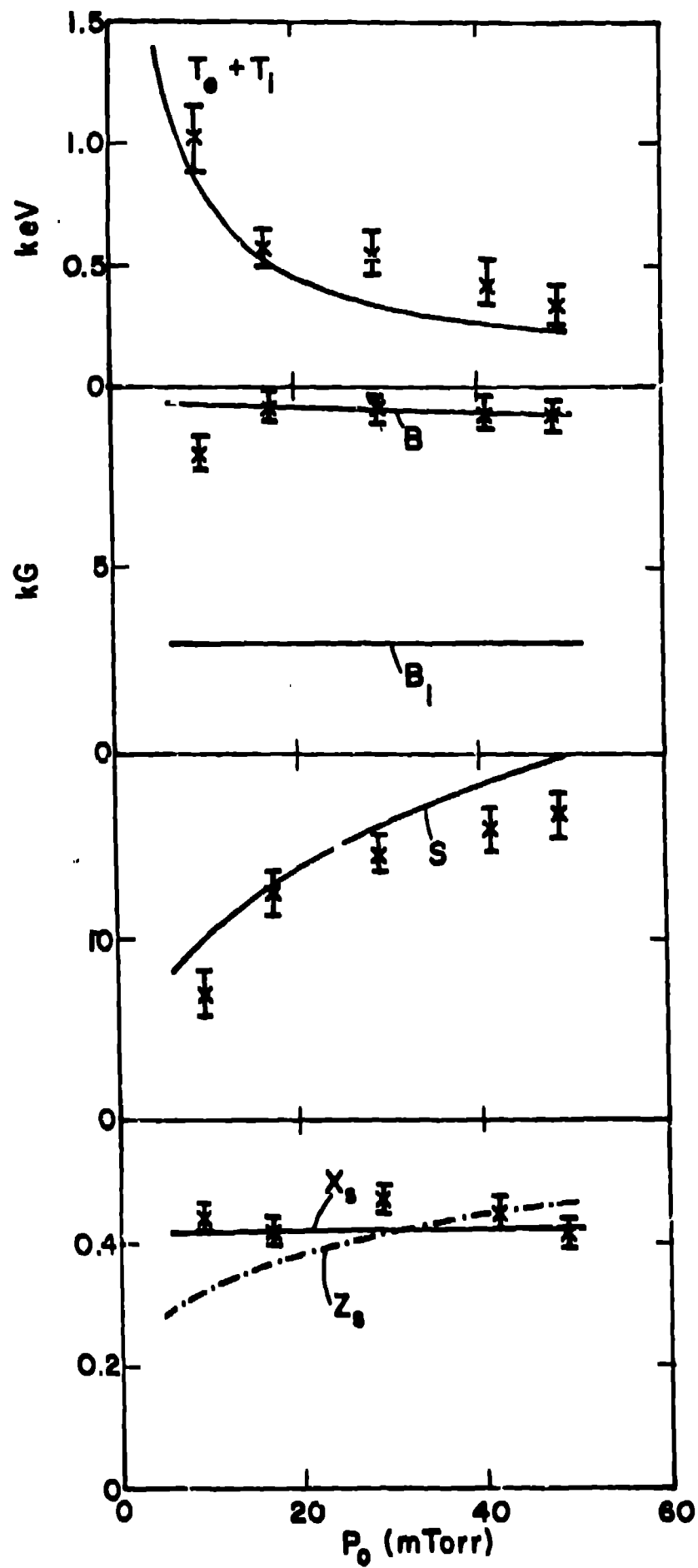


Fig. 4

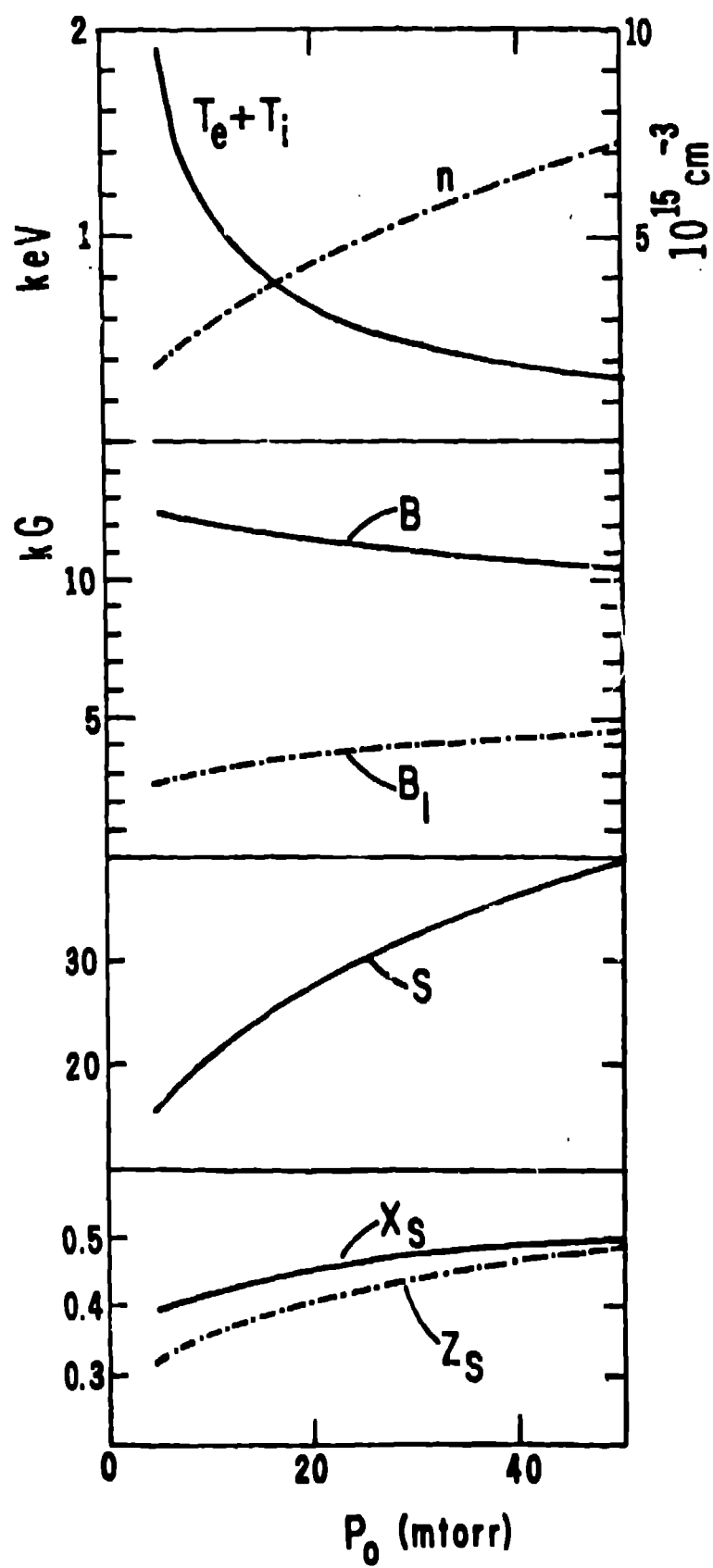


FIG. 5